Transactions of the Materials Research Society of Japan 30[1] 11-14 (2005)

Electronic Structure of Nd-doped $Bi_4Ti_3O_{12}$ Single Crystal Probed by Soft-X-Ray Emission Spectroscopy

Tohru Higuchi, Takashi Goto,* Yuji Noguchi,*,** Masaru Miyayama,*
Takeshi Hattori and Takeyo Tsukamoto

Department of Applied Physics, Tokyo University of Science, 1-3 Kagurazaka, Shinjuku, Tokyo 162-8601, Japan
* Research Center for Advanced Science and Technology, University of Tokyo, 4-6-1 Komaba, Meguro, Tokyo 153-8505, Japan
** PRESTO, Japan Science and Technology Corporation (JST), 4-6-1 Komaba, Meguro-ku, Tokyo 153-8505, Japan
Fax: 81-3-5228-8241, e-mail: higuchi@rs.kagu.tus.ac.jp

The electronic structure in the *a-b* plane of Nd-substituted $Bi_4Ti_3O_{12}$ ($Bi_{4-x}Nd_xTi_3O_{12}$) single crystal was studied by X-ray absorption spectroscopy (XAS) and soft-X-ray emission spectroscopy (SXES). The crystal-field splitting decreases with increasing Nd^{3+} concentration. The Ti 3*d* and O 2*p* partial densities of states in the valence band region were observed in O 1*s* and Ti 2*p* SXES spectra. The energy position of the Ti 3*d* state overlapped with that of the O 2*p* state, indicating the occurrence of the hybridization effect between the Ti 3*d* and O 2*p* states. The hybridization effect between Ti 3*d* and O 2*p* states increases with increasing Nd^{3+} concentration. These results indicate the change of the bond length between Ti and O ions in the *a-b* plane.

Key words: $Bi_{4-x}Nd_xTi_3O_{12}$, single crystal, soft-X-ray emission spectroscopy (SXES), electronic structure, hybridization

1. INTRODUCTION

Ferroelectric thin films have attracted considerable attention because of their use in ferroelectric random access memories (FeRAMs). Most attention has been focused on bismuth-layer-structured ferroelectrics, such as $Bi_4Ti_3O_{12}$ (BIT) and $SrBi_2Ta_2O_9$ [1-3]. However, the poor fatigue characteristic and the same remanent polarization of these ferroelectrics are viewed as the major problem in their FeRAM applications. Therefore, La-doped BIT ($Bi_{4-x}La_xTi_3O_{12}$) has been reported as a promising material for solving such problems. The $Bi_{4-x}La_xTi_3O_{12}$ thin film prepared at a low temperature of 650°C exhibits a relatively large remanent polarization and superior fatigue endurance [4-6]. Such a significant improvement in ferroelectricity has been observed only for $(Bi_{4-x}La_x)(Ti_{3-y}V_y)O_{12}$ and $Bi_4Ti_{3-y}V_yO_{12}$ films. This selective control of each site is called "site engineering". The site engineering effect on BIT has been extensively studied by Watanabe *et al.* and Tokumitsu *et al* [7-10]. They reported that the major contribution of site engineering to BIT is to the adjustment of the Curie temperature and the suppression of domain pinning. However, fundamental knowledge of the site-engineering effect for BIT is lacking. Therefore, understanding the electronic structure of BIT is also one of the most important considerations for its further applications.

In this study, the electronic structures of $Bi_{4-x}Nd_xTi_3O_{12}$ (BNT) single crystals have been investigated by high-resolution X-ray absorption spectroscopy (XAS) and soft-X-ray emission spectroscopy (SXES). It is generally known that photoemission spectroscopy (PES) is a powerful technique for the investigation of the electronic structure. The PES is surface sensitive and charging for insulator. Thus, it is difficult to study the electronic structure of a ferroelectric material by PES. SXES and XAS can confirm the electronic structure in the bulk state, because the mean free path of a soft-X-ray is very long compared with that of an electron. On the other hand, the SXES spectra, which have clear selection rules regarding the angular momentum due to dipole transition, reflect the occupied partial density-of-state (DOS). The XAS is related directly to the unoccupied DOS. This optical process is rather local process, because of the localized core state. It is governed by dipole selection rules so that XAS gives the spectrum related to the site- and symmetry-selected DOS.

2. EXPERIMENTAL

Powder samples of BNT were prepared by solid-state reaction. BNT single crystals were grown by a self-flux method using the BNT powder and Bi_2O_3 as a flux [11]. Nd^{3+} concentration (x) in the crystals was determined with inductively coupled plasma analysis. Time-of-flight neutron powder diffraction data were collected at 25°C using the Vega diffractometer [12]. Structural parameters were refined by the Rietvelt method using the program RIETAN-2001T based on B2cb orthorhombic symmetry [13].

XAS and SXES measurements were carried out at the revolver undulator beamline BL-19B at the Photon Factory of the High Energy Accelerator Organization, in Tsukuba, Japan. High brightness and high resolution were realized using a varied- line-spacing plane grating monochrometer. The XAS spectra were measured by a Si photodiode. The SXES spectra were measured by a soft-X-ray emission spectrometer. The spectrometer used the Rowland circle geometry that consisted of a grating with a groove density of 300 lines/mm and a Cs-coated multichannel detector. The total resolutions

of XAS and SXES were approximately 0.1 eV and 0.4 eV, respectively, at $h\nu$=450 eV.

In this measurement system, the incident angle of the soft-X-ray was approximately 70° in order to avoid the self-absorption effect. Figure 1 shows a schematic diagram of the experimental system. In this study, the SXES spectra were measured at the polarized configuration. As a reference, the depolarized configuration is also shown in this figure [16-18]. In the depolarized configuration, the polarization vector of the emitted photon (E_{out}) is rotated by 90° from the polarization vector of the incident photon (E_{in}). In the polarized configuration, the polarization vector of E_{out} contains the same polarization vector as that of E_{in}. Therefore, the SXES spectra at the polarized configuration reflect the electronic structure within the *a-b* plane.

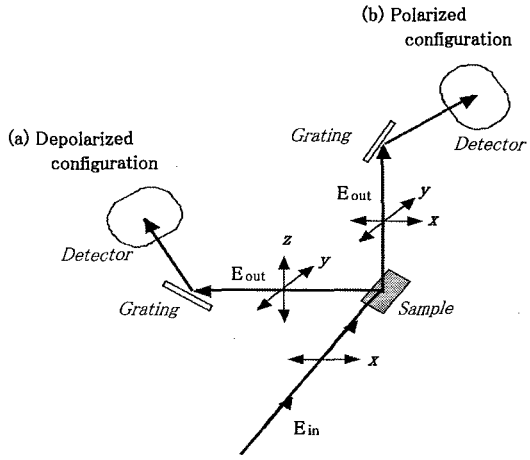

Fig. 1 Schematic diagrams of (a) depolarized and (b) polarized configurations for SXES. (a) Depolarized configuration: the spectrometer is located in the direction of the polarization vector of the incident photon (Ein). (b) Polarized configuration: the spectrometer is located normal to the wave vector and the polarization vector of E_{in}.

3. RESULTS AND DISCUSSION

Figure 2 shows Ti 2*p* XAS spectra in the *a-b* plane as a function of Nd^{3+} concentration in BNT single crystals. The Ti 2*p* XAS spectra correspond to the transition from the Ti 2*p* core level to the unoccupied Ti 3*d* state. The spectra are derived from the two parts of L_3 ($2p_{3/2}$) and L_2 ($2p_{1/2}$). They are split into the t_{2g}- and e_g-subbands by the octahedral ligand field [17,18]. The intensities of four peaks do not depend much on Nd^{3+} concentration, indicating that the substituted Nd^{3+} ions do not enter the Ti^{4+} site of BIT. The crystal-field splitting, which corresponds to the energy separation between t_{2g}- and e_g-subbands, decreases with increasing Nd^{3+} concentration. This result reflects the change of lattice constant in the *a-b* plane.

Figure 3 shows the O 1*s* and Ti 2*p* SXES spectra in the valence band region of BIT single crystal. The intensities of the SXES spectra are normalized by the beam current and measurement time. The clear selection rule of SXES is caused mainly within the same atomic species, because the core hole is strongly localized. For this reason, the O 1*s* and Ti 2*p* SXES spectra reflect the O 2*p* PDOS and Ti 3*d* PDOS, respectively. The energy position of O 2*p* state overlaps with that of Ti 3*d* state in the valence band. The valence band has two peaks, A and B, at –5.2 eV and –7.5 eV, respectively. Comparing both SXES spectra, the Ti 3*d* contribution is more significant on the higher energy side (peak B), where the O 2*p* state has a larger admixture of the Ti 3*d* state. On one hand, the valence band derived from the O 2*p* state hybridizes with the Ti 3*d* state. Thus, we estimate that the peak A corresponds to the nonbonding state and the peak B corresponds to the bonding state that is well mixed with Ti 3*d* state [17].

The PDOS histogram calculated in BIT is also shown under each SXES spectrum of Fig. 3. The electronic structure calculations based on the density functional

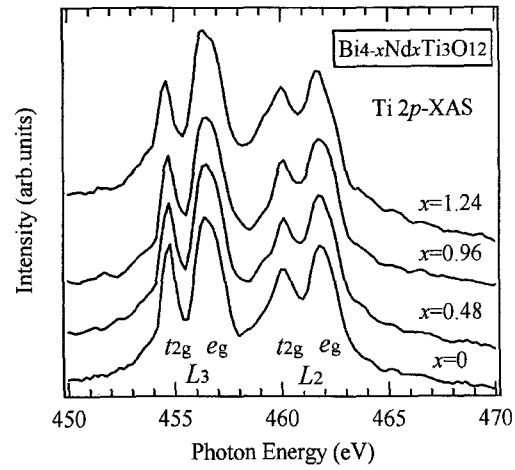

Fig. 2 Ti 2*p* XAS spectra as a function of Nd^{3+} concentration in BNT single crystals.

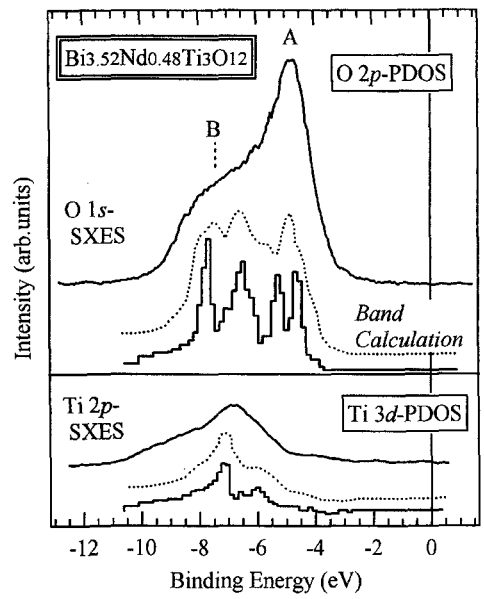

Fig. 3 O 1s and Ti 2p SXES spectra of BNT single crystal. For reference, the calculated band DOS is also shown under each SXES spectrum.

theory using local density approximation (LDA) were performed using the *ab-initio* calculation program. In order to calculate the electronic structure, we optimized the bases sets with effective core potential. A dashed curve above each calculated PDOS histogram is obtained by convoluting the original PDOS with Gaussian broadening functions with a width of 0.5 eV, which reflects the total resolution of the experimental system. The bandwidths and peak positions of the calculated PDOS are in good agreement with those of the Ti 2*p* and O 1*s* SXES spectra.

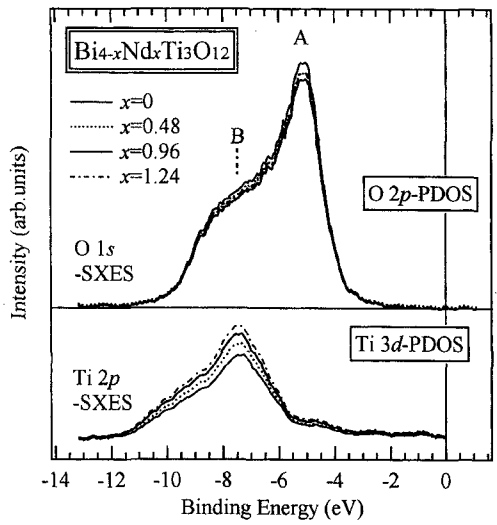

Fig. 4 O 1*s* and Ti 2*p* SXES spectra as functions of Nd^{3+} concentration in BNT single crystals.

Figure 4 shows the O 1*s* and Ti 2*p* SXES spectra as functions of Nd^{3+} concentration in BNT single crystals. The intensities of the SXES spectra are normalized by the intensity of the elastic scattering, although the elastic scattering peak is not shown in this figure. At all Nd^{3+} concentration, it is clear that the O 2*p* state hybridizes with the Ti 3*d* state in the valence band, as shown in the case of BIT single crystal in Fig. 3. The change of the bandwidth of the valence band is not observed in BNT single crystals. The intensity of the Ti 3*d* PDOS increases with increasing Nd^{3+} concentration. This result indicates that the hybridization effect between Ti 3*d* and O 2*p* states increases with increasing Nd^{3+} concentration. The change in the hybridization effect is considered to be due to the change in lattice constant or bond length between Ti and O ions in the *a-b* plane of BIT.

The above results indicate that the hybridization effect between Ti 3*d* and O 2*p* states is closely related with the ferroelectricity of BNT. Similar result has been reported in the ferroelecrics $BaTiO_3$ and $PbTiO_3$ [21,22]. The strong hybridization between Ti 3*d* and O 2*p* states increases the bonding energy of the Ti-O bond, enhancing the covalency of the bond. Since the covalent bond distance is ordinary shorter than the ionic bond length, the strong covalent interaction distorts the crystal structure, thus producing ferrolectric polarization of displactive-type ferroelecrtric materials [21].

In terms of crystal structure, the lattice constant of the *a*-axis in BNT decreases rapidly from 5.45 Å to 5.40 Å at $0 < x < 1.0$, although that of the *b*-axis decreases with Nd^{3+} concentration [23]. In other words, the bond length between Ti and O ions within the *a-b* plane decreases with increasing Nd^{3+} concentration. The above result concludes that the hybridization effect of BIT is closely related to the lattice constant or the bond length between Ti and O ions.

4. CONCLUSION

We have studied the electronic structure in the *a-b* plane of BNT single crystals using XAS and SXES. The 10Dq increases with decreasing Nd^{3+} concentration, indicating that the lattice constant in the *a-b* plane decreases with Nd^{3+} concentration. The valence band of BNT is mainly composed of O 2*p* state hybridized with Ti 3*d* state. The hybridization effect between the Ti 3*d* and O 2*p* states decreases with increasing Nd^{3+} concentration. These results conclude that the hybridization effect of BNT is closely related to the lattice constant and the bond length between Ti and O ions within the *a-b* plane.

ACKNOWLEDGEMENT

We would like to thank Prof. S. Shin for his useful discussion. This work was supported by a Grant-In-Aid for Scientific Research from the Ministry of Education, Culture, Sports, Science and Technology.

REFERENCES

[1] E. C. Subbarao: Phys. Rev. **122** (1961) 804.
[2] S. E. Cummins and L. E. Cross: Appl. Phys. Lett. **10** (1967) 14.
[3] R. W. Wolfe and R. E. Newnham: J. Electrochem. Soc. **116** (1967) 832.
[4] B. H. Park, B. S. Kang, S. D. Bu, T. W. Noh, J. Lee and W. Jo: Nature **410** (1999) 682.
[5] U. Chon, G. Yi and H. M. Jang: Appl. Phys. Lett. **78** (2001) 658.
[6] Y. Hou, X. Xu, H. Wang, M. Wang and S. Shang: Appl. Phys. Lett. **78** (2001) 1733.
[7] T. Watanabe, A. Saiki, K. Saito and H. Funakubo: J. Appl. Phys. **89** (2001) 3934.
[8] E. Tokumitsu, T. Isobe, T. Kijima and H. Ishiwara: Jpn. J. Appl. Phys. **40** (2001) 5576.
[9] T. Watanabe, T. Kojima, T. Sakai, H. Funakubo, M. Osada, Y. Noguchi and M. Miyayama: J. Appl. Phys. **92** (2002) 1518.
[10] T. Watanabe, H. Funakubo, M. Osada, Y. Noguchi and M. Miyayama: Appl. Phys. Lett. **80** (2002) 100.
[11] M. Soga, Y. Noguchi, and M. Miyayama, Trans. Mater. Res. Soc. Jpn. **28** (2003) 173.
[12] M. Takahashi, Y. Niguchi and M. Miyayama, Jpn. J. Appl. Phys. **42** (2003) 6222.
[13] T. Kamiyama, K. Oikawa, N. Tsuchiya, M. Osawa, H. Asano, N. Watanabe, M. Furusawa, S. Satoh, I. Fujikawa, T. Ishigaki, and F. Izumi, Physica B **213-214** (1995) 875.
[14] T. Ohta, F. Izumi, K. Oikawa, and T. Kamiyama,

Physica B **234-236** (1997) 1093.
[15] S. Shin, A. Agui, M. Fujisawa, Y. Tezuka, T. Ishii, and N. Hirai, Rev. Sci. Instrum. **66** (1995) 1584.
[16] T. Higuchi, T. Tsukamoto, M. Watanabe, M. M. Grush, T. A. Callcott, R. C. Perera, D. L. Ederer, Y. Tokura, Y. Harada, Y. Tezuka, and S. Shin, Phys. Rev. B **60** (1999) 7711.
[17] T. Higuchi, M. Tanaka, K. Kudoh, T. Takeuchi, Y. Harada, S. Shin, and T. Tsukamoto, Jpn. J. Appl. Phys. **40** (2001) 5803.
[18] T. Higuchi, T. Tsukamoto, K. Kobayashi, Y. Ishiwata, N. Sata, K. Hiramoto, M. Ishigame, and S. Shin, Phys. Rev. B **65** (2002) 33201.
[19] R. E. Cohen, Nature (London) **358** (1992) 136.
[20] T. Higuchi, T. Tsukamoto, K. Oka, T. Yokoya, Y. Tezuka, and S. Shin, Jpn. J. Appl. Phys. **38** (1999) 5667.
[21] T. Higuchi, K. Kudoh, T. Takeuchi, Y. Masuda, Y. Harada, S. Shin and T. Tsukamoto, Jpn. J. Appl. Phys. **41** (2002) 7195.
[22] T. Higuchi, Y. Moriuchi, Y. Noguchi, M. Miyayama, S. Shin and T. Tsukamoto, Jpn. J. Appl. Phys. **42** (2003) 6226.
[23] T. Goto, Y. Noguchi, M. Soga and M. Miyayama, in preparation.

(Received December 23, 2004; Accepted January 31, 2005)